Plant behaviour: a mathematical approach for understanding intra-plant communication

Fabio Tedone[1*,2], Emanuela Del Dottore[2*], Barbara Mazzolai[2], Pierangelo Marcati[1]

1 Department of Mathematics, Gran Sasso Science Institute, L'Aquila, Italy
2 Department of micro-biorobotics, Istituto Italiano di Tecnologia, Pontedera, Italy

* Corresponding author email: fabio.tedone@gssi.it; emanuela.deldottore@iit.it

Abstract

Plants are far from being passive organisms being able to exhibit complex behaviours in response to environmental stimuli. How these stimuli are combined, triggered and managed is still an open and complex issue in biology. Mathematical models have helped in understanding some of the pieces in the complexity of intra-plant communication, but a larger and brighter view, setting together multiple key processes, is still missing. This paper proposes a fully coupled system of nonlinear, non-autonomous, discontinuous, ordinary differential equations to describe with accuracy the adapting behaviour and growth of a single plant, by deeply analysing the main stimuli affecting plant behaviour. The proposed model was developed, and here sustained, with the knowledge at the state of the art; and validated with a comparison among numerical results and a wide number of biological data collected from the literature, demonstrating its robustness and reliability. From the proposed analysis it is also shown an emerging self-optimisation of internal resources and feedback stimuli, without the need for defining an optimisation function for the wellness of the plant. The model is ultimately able to highlight the stimulus-signal of the intra-communication in plant, and it can be expanded and adopted as useful tool at the crossroads of disciplines as mathematics, robotics, biology, for instance for validation of biological hypothesis, translation of biological principles into control strategies or resolution of combinatorial problems.

Author summary

Plants are able to adapt themselves to a wide range of conditions. The complexity and efficiency of this behaviour suggest a richness of signals exchanged that allowed scientists to talk about communication. Understanding this network of stimuli is an important challenge to increase biological knowledge as well as to adapt plant mechanisms to different research fields. To address this quest we developed a mathematical model able to describe what cues are fundamental in plant communication and how they interact each other.

1 Introduction

Plants have developed, over generations, the ability to adapt their resource allocation, foraging strategies and growth rates according to the environmental conditions that change over space and time [1]. Such ability to adjust internal processes and

morphology in response to the environmental changes is referred by biologists as plant behaviour [2], or plant plasticity [3].

In a more recent review, [4] redefined the definition of plant plasticity adding to the previous environment-induced stimuli, the ability of plants to live according to purposeful behaviours developed on the base of a sort of memory for some fitness optimisation. Moreover, according to the author, the large number of external stimuli and internal targets that the plant has to manage could be the reason of not placing critical functions in a single (or two) organ, like animals' heart or brain.

Hence, plants are able to trigger a network of different cues that control molecular signalling in different tissues, organs and the whole plant [5]. Decoupling and clearly understanding such signals are challenging tasks but of fundamental importance for plant behaviour analysis. According to the studies that better analysed plant behaviour [1] , intra-plant signals can be categorised into three main groups: I) *electric signals*, typically used by plants to stimulate a fast adaptation, as required for instance in case of some nutrient deficiency or wounds [6,7]; II) *oscillatory signals*, that are driven by the circadian clock, and direct the growth [8,9]; and III) *hormons*, like *auxin*, *citokin*, *giberellin*, which are typically messengers of stress conditions [10,11].

Towards the understanding of plant behaviour, several mathematical models have been proposed with the aim of analysing selected signalling pathways and internal dynamics. For example, in [12], a coupled PDE-ODE (Partial and Ordinary Differential Equation respectively) system describes the cross-talk between the *brassinosteroid* and *gibberellin* signalling pathways; while, other authors modelled the water uptake by roots and the associated morphology [13,14]. The fluid dynamics inside the xylem and phloem has been also of interest [15,16], as well as, the photosynthesis [17–20] and the interaction between different plants [21,22]. However, plant behaviour is determined by a very complex assembling of very different signals and to date none of the proposed models is able to describe such complexity and clearly discriminate stimulus-signal-behaviour chain in view of an internal communication network.

A previous tentative of analysing the mechanisms behind intra-plant communication has been done in [23], with the aim to identify and exploit basic biological principles for the analysis of plant roots behaviour. The analysis was carried in simulated environment and on robotic roots by translating the identified biological rules into algorithmic solutions. Particularly, on each root individually, the uptake kinetic and a local memory were used to adjust the local priority of nutrients, while the resources collected as a whole were shared according to the source-sink principle. Even if each root is acting independently from the others, just considering local information, results shown the emergence of a self-organising behaviour in plant roots aim at optimising the internal equilibrium among nutrients at the whole plant level, with no need for a central coordination or an optimisation function. However, in that work just a small part of the plant complexity was considered, for instance, it completely excluded the analysis of the above ground organs and photosynthesis-related dynamics.

In this paper, we do not aspire having a complete description of the plant complexity, yet we want to identify the main cues influencing the growth of a plant with the aim of investigating on the processes playing a role in the intra-communication for plant growth decisions. We propose and explain here a system of ODEs that, differently from the state of the art models, take into account the entire sequence of processes from nutrients uptake, photosynthesis and energy consumption and redistribution.

In particular, according to [24], biomass is an important estimator of plant fitness but it cannot be studied alone. For this reason, our model focuses on both above and below ground biomass, along with nutrients and sugar levels. In this way, it is possible to study independently leaves and roots adaptations to external and internal conditions. Moreover, unlike the most of existing models, it is possible to describe plant behaviour

when a more complete interaction among nutrients is taken into account. 57

We propose here a system of ODEs to outline the main cues influencing the growth 58
of a plant. In section 2 the model is described in details, emphasising the well proved 59
biological assumptions used to build up the equations. Section 3 presents several results 60
of numerical simulations and their comparison with the biological data obtained from 61
the literature, for validation of the model. Finally, in section 4 are discussed the key 62
elements of our model, its functionalities and the improvements with respect to the 63
state of the art, while section 5 presents conclusive remarks. 64

2   Methods 65

2.1   Description of the mathematical model 66

Through the photosynthesis, plants produce glucose from carbon dioxide and water, 67
using the energy from sunlight. To avoid starvation in the night, they should carefully 68
manage the resources acquired and produced during the day. Also, a plant is composed 69
by organs with different tasks. For instance, roots are the organs of the plant furnishing 70
water and nutrients to the above ground part, receiving from it the photosynthetic 71
products, particularly in the form of sugars, needed for growth and maintenance. While 72
the leaves are the energy producers and starch stores used during nights. According to 73
the resources availability and the energy produced, the biomass is differently distributed. 74

Nutrients are transported toward root surface mainly by water flow in soil. 75
Nevertheless, nutrient uptake is controlled by spatial distribution of roots. In fact, as 76
explained in [25], root system can develop to easily access to immobile nutrients (e.g. 77
phosphorus or ammonium), or locally adapt their exploitation power for a specific 78
nutrient. 79

According to [26], there are 17 most important nutrients for plants that can be 80
distinguished in two main categories: macronutrients (usually required in high 81
quantities) and micronutrients (which are required in smaller quantity). 82

As reviewed in [27], the nutrients content in soil should fall in specific ranges for the 83
plant not to suffer from toxicity or deficiency effects. Moreover, the same authors show 84
how an optimal ratio between nutrient contents in plant is necessary and how an 85
imbalance of such ratio can actively affect the uptake of nutrients. 86

Due to the complex network of interactions between nutrients, in both soil and plant, 87
usually only one nutrient [17, 20, 28], or the single water availability [14, 21, 29], have 88
been studied. 89

Some authors have studied an interaction between nutrients but avoiding a whole 90
plant interaction like photosynthesis or sugar-signalling [30]. 91

In our model, in order to study a more complete network of signals, over 92
sugar-signalling, we developed a root process dynamic model considering the presence of 93
two nutrients in the soil, and assuming a non-limiting and uniform distribution of water 94
in soil and of CO_2 in air. 95

For our study, we selected nitrogen (n) and phosphorus (p), being both fundamental 96
nutrients for growth in plants. 97

Nitrogen is the most abundant nutrient in plants, essential constituent of protein 98
and chlorophyll. Moreover it promotes root growth, improves fruit quality, enhances the 99
growth of leafy vegetables, increases protein content of fodder, encourages the uptake 100
and utilisation of other nutrients [31]. 101

Phosphorus is essential for growth, cell division, root lengthening, seed and fruit 102
development, and early ripening. It is a part of several compounds including oils and 103
amino acids. The P compounds adenosine diphosphate (ADP) and adenosine 104
triphosphate (ATP) act as energy carriers within the plant [32]. 105

The proposed model takes in consideration all these fundamental working principles, by describing the dynamics of each actor: photosynthesis, starch, sucrose, nutrients uptake and management, costs of maintenance and growth, and biomass allocation.

For the sake of simplicity, the time dependence of functions and variables is implied and it will not be reported in the following model equations.

2.2 Photosynthesis

We described the photosynthesis ($[\frac{\mu mol C_6}{gFW \cdot h}]$) process with a time-dependent function describing the content of sugar produced by each gram of photosynthetically active leaf biomass:

$$p_h = LCp_h^{max}min(n_t, p_t) \tag{1}$$

where:

- L $[-]$ is a binary function to distinguish day by night. It is 1 during day and 0 during night. It should be noted that L can be easily modified in a continuous time-dependent function assuming values in the range $[0, 1]$, so to consider temperature and light intensity effects.

- C $[-]$ is a positive function in the range $[0, 1]$. It represents a limiting coefficient to photosynthesis dependent on the plant status. In fact, different saturating processes can affect stomatal conductance, reducing photosynthesis production ([33] reviewed many modelling approaches). Particularly, [34] suggests a more specific photosynthesis limiting process, which is indirectly linked to the need of the plant of avoiding the production of starch and sugar in excess. Accordingly to [35] and [20], we propose a limiting function depending on the maximum starch that the plant can consume in nightly hours. The C function can be written as:

$$C = \lambda_c + (1 - \lambda_c)(\frac{a_{max} - a}{a_{max}}) \tag{2}$$

where:

$$a_{max} = \tau_{as}^{max}(24 - f) \tag{3}$$

The parameter λ_c describes the strength of photosynthesis limitation, a is the starch, a_{max} the maximum starch that can be consumed at the maximum rate τ_{as}^{max} during the night and f the photo-period. The sugar limitation will affect the starch partition (γ) dynamics, that will be explained later (Section 2.3.2).

- p_h^{max} $[\frac{\mu mol C_6}{gFW \cdot h}]$ is the maximum rate of photosynthesis. As for in [36], it is fixed to $12.7\frac{\mu mol C_6}{gFW \cdot h}$.

- n_t and p_t represent nitrogen and phosphorus saturating threshold, respectively. Both these nutrients play a role in the photosynthesis process (see [37] for an explanation of the role of nitrogen, while [38] reviews phosphorus influence on photosynthesis). Hence, photosynthesis is strictly correlated with nutrient availability in a saturating way. In fact, according to the law of minimum [39], the most limiting nutrient content will mainly affect the photosynthesis. By [17], the rate of carbon production obtained from nitrogen content is estimated as:

$$15.44\frac{gC}{gN \cdot h} = 2.21\frac{\mu mol C_6}{\mu mol N \cdot h} \tag{4}$$

Hence, the minimum nitrogen content required to sustain the maximum rate of photosynthesis is:

$$n_{ph} = \frac{12.7}{2.21} = 5.75 \frac{\mu mol N}{gFW} \tag{5}$$

The saturating function n_t can be computed as:

$$n_t = \frac{n}{n + n_{ph}} \tag{6}$$

Not having found similar information for phosphorus, we estimated the saturating function of this nutrient by assuming the consumption of phosphorus as one-tenth of the nitrogen's one, according to the optimal ratio among these two nutrients, which has been observed to be about 10 (as reviewed in [23]). Therefore, we approximated:

$$p_{ph} = \frac{n_{ph}}{10} \tag{7}$$

$$p_t = \frac{p}{p + p_{ph}} \tag{8}$$

where $n \; [\frac{\mu mol N}{gFW}]$ and $p \; [\frac{\mu mol P}{gFW}]$ are respectively the nitrogen and phosphorus content.

In particular, if $n < n_{ph}$ or $p < p_{ph}$, then it should be $n_t = 0$ or $p_t = 0$ respectively just because there are not enough resources to start the chemical processes.

It should be noted that Eq (1) is a simplification of the more general formula:

$$p_h = LC p_h^{max} min(n_t, p_t) \frac{min(b_l^{max}, b_l)}{b_l} \tag{9}$$

which takes into account the aboveground biomass (b_l) and the maximum photosynthetically active leaf biomass (b_l^{max}). However, since in all papers used for validation there was no clue that the critical biomass was reached during the experiments, the b_l^{max} is assumed to be infinite, allowing us to remove the biomass factorial term.

2.3 Starch and Sucrose

During the day, some photosynthate is stored as starch to be degraded during night to sustain the nocturnal metabolism. Independently by the length of the night, the starch is degraded into sucrose in a nearly linear manner (at a rate τ_{as}), such that almost all of the starch is used by dawn [40]. We described starch and sucrose dynamics with the equations:

$$\frac{da}{dt} = \gamma p_h - \tau_{as} \tag{10}$$

$$\frac{ds}{dt} = (1 - \gamma) p_h + \tau_{as} - r_m^u - r_m^t - r_m s - \eta r_g \tag{11}$$

A very similar dynamic can be found in [41] and [42]. Nevertheless, some important differences deserved to be outlined:

- The photosynthesis p_h in the current model is not a constant, but it is a time-dependent function parametrized on nutrient availability, light, sugar-signalling and leaf competition (as described in previous section);

- The starch partition coefficient γ is not a constant, neither it is estimated assuming sucrose homoeostasis (as in the model of [43]). It provides instead plant adaptation as a function of time (its dynamic is described in Section 2.3.2); 145 146 147

- The starch degradation rate τ_{as} is simpler respect to the definition provided in [41] and [42], and it does not depend on a subjective dusk [44]. Even considering the simplification adopted in this paper for starch degradation, its dynamic remains correct (see file S1 in supporting information for demonstration); 148 149 150 151

- Just like in [20], both uptake (r_m^u) and transport (r_m^t) processes are sucrose consuming, over the usual maintenance respiration (r_m); 152 153

- The rate of sucrose sent into the phloem intended for growth (ηr_g) is affected by nocturnal efficiency [45]. 154 155

2.3.1 Starch degradation 156

It is well established that maintenance and growth respiration occur both during day and night. The sucrose to sustain nightly metabolism is provided by the degradation ($[\frac{\mu mol C_6}{gFW \cdot h}]$) of starch stored in the morning [40], and here defined as:

$$\tau_{as} = (1 - L)min(\tau_{as}^{max}, (\frac{t}{24} + (1 - \frac{t}{24})(1 - \frac{s}{s + s^{max}}))\frac{a_{|dusk} - a^{min}}{24 - f}) \qquad (12)$$

where: 157

- $\tau_{as}^{max} = 6 \frac{\mu mol C_6}{gFW \cdot h}$ is the maximum degradation rate estimated by the results shown in [36]; 158 159

- $s^{max} = 2 \frac{\mu mol C_6}{gFW}$ is the maximum sucrose content in leaves. It is estimated by experimental values in [46]. A negative feedback on starch degradation due to high sucrose levels is proposed also in [47]. Hence, the introduction of a maximum threshold is justified by these evidences. On the other hand, a minimum threshold should be expected to trigger sugar production or starch degradation in case of starvation. Like in [36], s^{min} is estimated as $1.3\frac{\mu mol C_6}{gFW}$; 160 161 162 163 164 165

- $a_{|dusk}$ $[\frac{\mu mol C_6}{gFW}]$ is the starch content at the beginning of the night. The use of this parameter makes us highlight some differences with respect to the model presented in [41], where: I) the function proposed to describe starch degradation is independent from this parameter and has a peak at dawn; II) starch degradation is assumed to exist also during the light period; and III) the non linear discontinuous function proposed takes into account the surface of starch granule. In the supporting material, we integrated their function in our model and we compared the two approaches; 166 167 168 169 170 171 172 173

- $a_{min} = 0.15 \frac{\mu mol C_6}{gFW}$ is the minimum amount of starch that plant has to ensure. It is estimated by [41]. 174 175

Hence, during night ($L = 0$), the starch is degraded with a rate that depends both on the time t with respect to the next expected dawn (circadian clock), the sucrose signalling and the constant rate necessary to consume almost all of the starch by dawn. This strategy holds unless the required rate is greater than the maximum one. 176 177 178 179

2.3.2   Starch and sucrose partitioning

[47] explains how rising levels of sucrose stimulate starch synthesis, while daily sucrose starvation decreases starch accumulation. Nightly sucrose starvation, on the other hand, promotes starch production [20]. From these observations, we defined the dynamic of starch-sucrose partitioning as:

$$\frac{d\gamma}{dt} = L(-\gamma\lambda_{sdr}\frac{s^{min}}{s^{min}+s} + (1-\gamma)\lambda_{sdi}\frac{s}{s+s^{max}}) + (1-L)(1-\gamma)\lambda_{sni}\frac{s^{min}}{s^{min}+s} \quad (13)$$

2.4   Biomass allocation

Sucrose transport is essential to allow growth and maintenance of non photosynthetically active tissues like roots, shaded and/or young leaves, and other storage organs [48]. Actually, the sucrose is loaded into phloem generating an osmotic pressure which drives both water and sucrose from source tissues to sinks [49].

In particular, testing Münch hypothesis, [50] shows a sink priority concept affecting how sucrose loaded is allocated between sinks. In our model, sucrose is divided between above and below ground biomass. The partitioning coefficient f_r of sucrose allocated to roots is described by the following equation:

$$\frac{df_r}{dt} = (1-f_r)(a_n f_n + (1-f_n)a_p) - f_r(\frac{nf_n}{n+n^{min}} + \frac{p(1-f_n)}{p+p^{min}} + \frac{s^{min}}{s+s^{min}}) \quad (14)$$

where $f_n = \frac{10}{10+\frac{n}{p}}$ is a stoichiometry signal with respect to the optimal nutrient ratio. The frequency parameter fixed to $1\frac{1}{h}$ is omitted in the previous equation.

According to [51], the less nutrients are, the more root priority is and vice versa. In particular, [52] stresses that sink priority is affected by the most limiting resource, while [53] and [54] highlight how plants are able to adapt their allocation strategies according to internal and external stimuli. Hence, while functions a_n and a_p describe nutrients demand, the value of s with respect to the threshold s^{min} describes a limitation due to leaves.

As result, the function f_r balances the nutrients demand with respect to the most limiting resource, and describes the sucrose allocation between leaves and roots. Moreover, being a central brain missing in plant, there is not central control on carbohydrates allocation, thus we hypothesis a different nutrient feedback driving resources allocation within roots (the same hypothesis should be valid for leaves, but we are not interested in modelling spatial distribution of leaves at this stage of the work).

According to [55], [51] and [56], the innate soil heterogeneity affects root system morphology promoting root proliferation in nutrient-rich soils. In our model the choice is between two different soil zones. Given sucrose allocated to roots, the proportion of resources sustaining growth in the top soil is given by the following weighted average ([−])

$$e_1 = \frac{f_n n_{s1}}{n_{s1} + n_{s2}\chi_1} + \frac{(1-f_n)p_{s1}}{p_{s1} + p_{s2}\chi_1} \quad (15)$$

Being soil zones vertically distributed, the binary function χ_1 is necessary to express if the root biomass has reached the second (deeper) soil zone. Actually, χ_1 is 1 if $b_{r1} > b_r^c$, where b_r^c is a parameter describing the critical biomass to reach before having access to the deeper zone.

2.5 Growth

Considering the above observations on biomass allocation, we can describe the growth dynamics of leaves and roots with the equations:

$$\frac{db_l}{dt} = \lambda_{sb}(1 - f_r)\eta r_g b_l min(\frac{b_l^{max}}{b_l}, 1) \tag{16}$$

$$\frac{db_{r1}}{dt} = \lambda_{sb}e_1 f_r \eta r_g b_l min(\frac{b_l^{max}}{b_l}, 1) \tag{17}$$

$$\frac{db_{r2}}{dt} = \lambda_{sb}(1 - e_1)f_r \eta r_g b_l min(\frac{b_l^{max}}{b_l}, 1) \tag{18}$$

In Eq (16), (17) and (18), λ_{sb} is a conversion parameter from sucrose to biomass. The growth, according to the specific tissue priority (f_r and e_1), will be proportional to the whole sucrose exported by photosynthetically active leaf biomass.

2.6 Nutrients dynamics

To study the root system adaptation in a changing environment, we assumed the soil divided into two zones: the topsoil and the subsoil. This choice is justified by the different mobility of phosphorus and nitrogen (the selected nutrients for our study). The former is immobile and usually a greater content can be found in topsoil [57]. Nitrogen, on the other hand, is quite mobile and easily transported by percolating water in subsoil [58,59].

We described the plant dynamics of nitrogen n $[\frac{\mu mol N}{gFW}]$ and phosphorus p $[\frac{\mu mol P}{gFW}]$ content as:

$$\frac{dn}{dt} = u_n - (r_m(s + a) + \eta r_g)c_{sn}\frac{min(b_l^{max}, b_l)}{B} - \frac{p_h}{p_h^{max}}n_{ph}\lambda_f \tag{19}$$

$$\frac{dp}{dt} = u_p - (r_m(s + a) + \eta r_g)c_{sp}\frac{min(b_l^{max}, b_l)}{B} - \frac{p_h}{p_h^{max}}p_{ph}\lambda_f \tag{20}$$

u_n $[\frac{\mu mol N}{gFW \cdot h}]$ and u_p $[\frac{\mu mol P}{gFW \cdot h}]$ are the nitrogen and phosphorus uptake rate, respectively (see Section 2.6.1 for details).

In [17], the cost of assimilating n into biomass is estimated as $r_A = 4.06\frac{gC}{gN} = 0.58\frac{\mu mol C_6}{\mu mol N}$. Hence the n cost of assimilating C_6 can be estimated as proportional to:

$$c_{sn} = \lambda_{csn}1.724\frac{\mu mol N}{\mu mol C_6} \tag{21}$$

As already previously justified (Section 2.2), the p cost of assimilating C_6 can be approximated using the optimal ratio value ([23]) as $c_{sp} = \frac{c_{sn}}{10}$. In particular, metabolism, transport and growth will be reduced if the nutrient content is not sufficient to sustain the costs (c_{sn} and c_{sp}). Then:

$$\chi_{np} = min(1, \frac{n}{s^{max}c_{sn}})min(1, \frac{p}{s^{max}c_{sp}}) \tag{22}$$

$$r_m = r_m\chi_{np} \tag{23}$$

$$r_g = r_g\chi_{np} \tag{24}$$

The second terms of Eq (19) and (20) are the n and p costs owed to the use of sucrose for maintenance and growth. Also, the starch requires a maintenance respiration (and then a cost in nutrients) due to the production of storage structures [60].

Note that s and a represent the quantity of moles of C_6 for each gram of photosynthetically active leaf biomass. Then, the term $\frac{min(b_l^{max}, b_l)}{B}$ is necessary to consider the actual plant sugar content, being B the full plant biomass.

Finally, the last terms of Eq (19) and (20) express the nutrient costs due to photosynthesis. Knowing the nutrient cost for the maximum rate, n_{ph} (Eq (5)) and p_{ph} (Eq (7)), the actual consume will be proportional to the intensity of photosynthesis. The frequency parameter λ_f $[\frac{1}{h}]$ will be estimated later (Section 2.9).

2.6.1 Nutrients uptake

Having nutrients located in two discrete soil zones, we described the potential uptake with two terms (labelled in subscript with index 1 - topsoil - and 2 - subsoil), each multiplied by a factor that takes into account the whole biomass. For nitrogen (and similarly for phosphorus) we defined:

$$u_n^{pot} = (u_{n1} \frac{min(b_{r1}^{max}, b_{r1})}{B} + u_{n2} \frac{min(b_{r2}^{max}, b_{r2})}{B})a_n \qquad (25)$$

where b_{r1} is the root biomass in topsoil, b_{r2} the root biomass in subsoil. b_{r1}^{max} and b_{r2}^{max} are the maximum root biomass allowed in each soil zone. As for b_l^{max} (in Eq (9)), we fix to infinite their value, assuming no root competition. a_n is an internal feedback explained later.

A limiting factor $[-]$ should be taken into account. Its role is to decrease the forage if the hourly potential uptake u_n^{pot} needs excessive sugar consumption with respect to the available one. Thus:

$$u_n^{real} = u_n^{pot} \frac{s}{s + n_c u_n^{pot} \cdot 1h} \qquad (26)$$

u_{n1} and u_{n2} $[\frac{\mu mol N}{gFW \cdot h}]$ are the nutrient rates of uptake, while n_c will be estimated later. It is well established that the uptake follows a Michaelis-Menten kinetics [61,62]:

$$u_{n1} = I_n^{max} \frac{n_{s1}}{n_{s1} + k_n} \qquad (27)$$

I_n^{max} $[\frac{\mu mol N}{gFW \cdot h}]$ is the nutrient maximum uptake, k_n $[\frac{\mu mol N}{cm^3}]$ is the Michaelis Menten constant and n_{s1} $[\frac{\mu mol N}{cm^3}]$ is a time depending function describing the nutrient content in the soil zone. Similar equations are defined for u_{n2} and phosphorus in top and subsoil.

Several papers have shown how Michaelis Menten parameters are not fixed [63–65]. Plants, in fact, are able to modify these parameters to be more or less affine with the specific nutrient. This adaptive behaviour is experimentally measured changing nutrient soil content [66].

However, [55] notes how changes in kinetics parameters could be due to plant internal status instead of environmental reasons. In particular, [55] reports how root proliferation and uptake require varying energies, and how the balance between costs and gains could explains the plant strategy.

In our model we tried to describe this behaviour. For this reason, from [67] we estimated kinetic parameters for nitrate, and from [63] we approximates phosphorus

parameters:

$$I_n^{max} = 6.44 \frac{\mu mol N}{gFW \cdot h}$$

$$k_n = 0.125 \frac{\mu mol N}{cm^3}$$

$$I_p^{max} = 0.4 \frac{\mu mol P}{gFW \cdot h}$$

$$k_p = 0.006736 \frac{\mu mol N}{cm^3}$$

They represent the maximum values for the couple (I^{max}, k). To simulate the nutrient affinity adaptation we introduced in Eq (25) the internal control a_n $[-]$. An analogous control a_p is inserted for phosphorus dynamics

$$u_p^{pot} = (u_{p1} \frac{min(b_{r1}^{max}, b_{r1})}{B} + u_{p2} \frac{min(b_{r2}^{max}, b_{r2})}{B})a_p \qquad (28)$$

Both a_p and a_n are positive time dependent functions bounded by 1. Their dynamics are described below (again the frequency parameter fixed to $1\frac{1}{h}$ is omitted in both the following equations):

$$\frac{da_n}{dt} = (1 - a_n)((1 - \frac{u_n}{u_n + C_n})\frac{n^{max}}{n^{max} + n} + \frac{p_h}{p_h^{max}} - a_n\lambda_k\frac{n - 10p}{n + 10p}) -$$
$$-a_n(\frac{n}{n + n^{min}} + \frac{n_c u_n}{n_c u_n + p_h(1 - \gamma) + \tau_{as}}) \qquad (29)$$

A similar formulation holds for the phosphorus control function a_p:

$$\frac{da_p}{dt} = (1 - a_p)((1 - \frac{u_p}{u_p + C_p})\frac{p^{max}}{p^{max} + p} + \frac{p_h}{p_h^{max}} + a_p\lambda_k\frac{n - 10p}{n + 10p}) -$$
$$-a_p(\frac{p}{p + p^{min}} + \frac{p_c u_p}{p_c u_p + p_h(1 - \gamma) + \tau_{as}}) \qquad (30)$$

C_n and C_p represent the nitrogen and phosphorus costs due to the actual strategy. They are the absolute value of the sum of the second and third terms in Eq (19) and (20).

n^{max} and p^{max} take into account the memory of a plant. In fact, according to [18], plants manage its foraging strategies in order to avoid both scarcity and excess of nutrients in stores. In particular, the optimal nutrient status is defined by how many days plant can survive maintaining the same rate of growth if a specific nutrient is not available anymore. [18] estimated for herbaceous plants (like *Arabidopsis*) a memory of 4 days. We fixed $D = 4$ $[-]$. Hence, the minimum amount of nitrogen content ($[\frac{\mu mol N}{gFW}]$) required to sustain photosynthesis and respiration for one day at the maximum sugar content is:

$$n^{min} = ((r_m(s^{max} + a^{max}) + \eta s^{max})(1 + 0.035)c_{sn}24 + n_{ph}\lambda_f f) \qquad (31)$$

Then, we estimated $n^{max} = Dn^{min}$ and $p^{max} = \frac{n^{max}}{10}$. The term:

$$(1 - \frac{u_n}{u_n + C_n})\frac{n^{max}}{n^{max} + n}$$

describes the active incentive for the uptake rate according to the internal status and the cost-gain balance as reported in [55]. On the other hand, the last terms in Eq (29) and (30) represent the active limitation to the uptake due to the same concepts.

Moreover, as emphasised by [68], over an active control of nutrient affinity, the uptake rate is passively increased by photosynthesis and leaves transpiration. The term:

$$\frac{p_h}{p_h^{max}} \tag{32}$$

describes this behaviour.

2.7 Costs

All the sucrose s produced by photosynthesis and starch degradation is used for maintenance and growth respiration costs.

As in [42], we assumed the respiration to be proportional to the sucrose content. The former has a frequency of $r_m = 0.79\frac{1}{h}$. The frequency of sucrose loaded into phloem for growth has a frequency of $\eta = 1.98\frac{1}{h}$. However, as observed in [45], the nightly starvation reduces the growth rate. To take into account this negative feedback, we reduced r_g under the parameter γ that in the model describes the nightly efficiency of starch. Hence:

$$r_g = s(\lambda_g + (1 - \lambda_g)(1 - L + L(1 - \gamma))) \tag{33}$$

The more γ increases, the more r_g decreases. Over maintenance and growth respiration, sucrose is consumed for the transport of carbon along the plant and for the uptake of nutrients. [20] estimates costs of uptaking phosphorus as:

$$p_c = 0.053\frac{\mu g Sugar}{\mu g P} = 0.308\frac{\mu mol C_6}{\mu mol P}$$

with a sugar transport cost of 0.035 [−] (carbon consumed for each gram of carbon allocated in phloem). The cost of uptaking nitrogen (n_c) is assumed, in our model, to be the same of phosphorus (p_c), being the uptake mechanism similar among all chemical elements. Hence:

$$n_c = 0.053\frac{\mu g Sugar}{\mu g N} = 0.68\frac{\mu mol C_6}{\mu mol N}$$

Named u_p [$\frac{\mu mol P}{gFW \cdot h}$] and u_n [$\frac{\mu mol N}{gFW \cdot h}$] the phosphorus and nitrogen rates of uptake respectively, the whole uptake (r_m^u) and transport (r_m^t) costs are:

$$r_m^u = n_c u_n + p_c u_p \tag{34}$$
$$r_m^t = 0.035(r_m s + \eta r_g) \tag{35}$$

2.8 Further environmental contributes

Additionally, we should consider how deficiency or excess of nutrients in soil affect plant behaviour. For instance, [69] shows how in nutrient-poor soils, the secondary metabolism and the plant defence overcome the growth stimulus. For this reason, it is important to quantify nutrient excess or deficiency with respect to an optimal threshold. In [70] for free N medium the value of $12\frac{\mu mol N}{cm^3}$ is used, and this value is used as optimal threshold in our model for nitrogen. [66] defined treatments in low P content up to $0.1\frac{\mu mol P}{cm^3}$, while treatments in high P content start from $0.2\frac{\mu mol P}{cm^3}$. Hence, we fixed the optimal value for phosphorus to $0.15\frac{\mu mol P}{cm^3}$. Therefore, the excess or deficiency will be measured with respect to the distance from the defined optimal thresholds and the

amount of relative roots that are experiencing it:

$$n_s = \frac{n_{s1}b_{r1} + n_{s2}b_{r2}}{(b_{r1} + b_{r2})} \frac{1}{12} \tag{36}$$

$$p_s = \frac{p_{s1}b_{r1} + p_{s2}b_{r2}}{(b_{r1} + b_{r2})} \frac{1}{0.15} \tag{37}$$

The increased defence-signal can be simulated limiting the conversion parameter λ_{sb}, and the increased metabolism will lead to greater nutrient stocks. We can simulate it increasing n^{min} and p^{min}. Both N and P are primary for plant growth and a negative feedback should be present to consider their combined effect.

The function R^- (defined in Eq (38)) is used to reduce λ_{sb}, regulating this way toxicity conditions, and it is symmetric with respect to n_s and p_s, with its maximum in $(n_s, p_s) = (1, 1)$. Moreover it is null if both nitrogen and phosphorus are missing in soil $((n_s, p_s) = (0, 0))$, while all negative values are also cut to 0.

$$R^- = -\frac{1}{2}(n_s^2 + p_s^2) + (n_s + p_s) \tag{38}$$

Hence:

$$\lambda_{sb} = \begin{cases} \lambda_{sb} R^-(n_s, p_s) & min(n_s, p_s) < 1 \\ \lambda_{sb} & min(n_s, p_s) \geq 1 \end{cases} \tag{39}$$

The function R^+ is instead used to increase nutrient demand, to regulate deficiency conditions in soil, and it is again symmetric and positive. It has one minimum $R^+(1, 1) = 1$ and an arbitrary value was fixed for $R^+(0, 0) = 139$. Hence:

$$R^+ = 69(n_s^2 + p_s^2) - 138(n_s + p_s) + 139 \tag{40}$$

and

$$n^{min} = n^{min} R^+(n_s, p_s) \tag{41}$$

$$p^{min} = p^{min} R^+(n_s, p_s) \tag{42}$$

where $R^+(n_s, p_s) = 1$ if $min(n_s, p_s) \geq 1$.

Fig 1. Reduction functions.
(A) Example of R^- function nitrogen or phosphorus soil content is less than the optimal one. (B) Example of R^+ function when nitrogen or phosphorus are deficient in soil.

Going over toxicity levels of nutrients, it will induce negative feedback in plant internal processes. For instance, excess of some forms of nitrogen can change soil pH making phosphorus more available [71]. Other forms of nitrogen can modify the C:N soil stoichiometry and stimulate a greater demand of other micro-nutrients (with possible negative effects) [71]. Moreover, the high nitrogen content in plant can increase the secondary metabolism instead of growth [69]. Other examples come for the phosphorus. According to [71], an high phosphorus content in soil can promote the luxury uptake of P. The plant absorbs more P than it needs modifying P:Fe and P:Zn stoichiometry ratios in plant. Consequences are the same of a Fe and Zn deficiency.

As case study, we wanted to include in our model the plant behaviour in case of luxury levels of P. To this aim, we should insert new equations for Fe and Zn dynamics and consequently more parameters to estimate optimal stoichiometry ratio. However, these data are not easily available in the literature. Hence, we introduced in the model a function simulating Fe deficiency when P content overcomes an optimal threshold.

Iron is fundamental in many metabolic pathways and photosynthetic organs. In fact, [72] shows how Fe deficiency affects the development of chlorophyll, limiting the rate of photosynthesis. In the paper, the authors conduct some experiments pointing out the strength of this inhibition. It can induce up to a 50% decrement in chlorophyll accumulation. Moreover, [72] explains that is not possible to induce a greater decrement. Hence, if $p_s \geq 1$, the maximum photosynthesis is reduced depending on the amount of phosphorus excess, according to the following:

$$p_h^{max} = \frac{12.7}{2}(1 + e^{1-p_s}) \tag{43}$$

If there is no excess, the photosynthesis does not experience any limitation ($p_h^{max} = 12.7$). The more excess, the more reduction occurs till the 50%.

2.9 Model overview and parameters

Summarising, the model is composed by 11 non-linear equations:

$$\frac{da}{dt} = \gamma p_h - \tau_{as}$$

$$\frac{ds}{dt} = (1-\gamma)p_h + \tau_{as} - r_m^u - r_m^t - r_m s - \eta r_g$$

$$\frac{d\gamma}{dt} = L(-\gamma\lambda_{sdr}\frac{s^{min}}{s^{min}+s} + (1-\gamma)\lambda_{sdi}\frac{s}{s+s^{max}}) + (1-L)(1-\gamma)\lambda_{sni}\frac{s^{min}}{s^{min}+s}$$

$$\frac{dn}{dt} = u_n - (r_m(s+a)+\eta r_g)c_{sn}\frac{min(b_l^{max},b_l)}{B} - \frac{p_h}{p_h^{max}}n_{ph}\lambda_f$$

$$\frac{dp}{dt} = u_p - (r_m(s+a)+\eta r_g)c_{sp}\frac{min(b_l^{max},b_l)}{B} - \frac{p_h}{p_h^{max}}p_{ph}\lambda_f$$

$$\frac{da_n}{dt} = (1-a_n)((1-\frac{u_n}{u_n+C_n})\frac{n^{max}}{n^{max}+n} + \frac{p_h}{p_h^{max}} - a_n\lambda_k\frac{n-10p}{n+10p})-$$
$$-a_n(\frac{n}{n+n^{min}} + \frac{n_c u_n}{n_c u_n + p_h(1-\gamma)+\tau_{as}})$$

$$\frac{da_p}{dt} = (1-a_p)((1-\frac{u_p}{u_p+C_p})\frac{p^{max}}{p^{max}+p} + \frac{p_h}{p_h^{max}} + a_p\lambda_k\frac{n-10p}{n+10p})-$$
$$-a_p(\frac{p}{p+p^{min}} + \frac{p_c u_p}{p_c u_p + p_h(1-\gamma)+\tau_{as}})$$

$$\frac{df_r}{dt} = (1-f_r)(a_n f_n + (1-f_n)a_p) - f_r(\frac{n f_n}{n+n^{min}} + \frac{p(1-f_n)}{p+p^{min}} + \frac{s^{min}}{s+s^{min}})$$

$$\frac{db_l}{dt} = \lambda_{sb}(1-f_r)\eta r_g b_l min(\frac{b_l^{max}}{b_l},1)$$

$$\frac{db_{r1}}{dt} = \lambda_{sb}e_1 f_r \eta r_g b_l min(\frac{b_l^{max}}{b_l},1)$$

$$\frac{db_{r2}}{dt} = \lambda_{sb}(1-e_1)f_r \eta r_g b_l min(\frac{b_l^{max}}{b_l},1)$$

Many model coefficients have been estimated by the literature, as already deeply described in the sections above. The remaining free parameters are:

- λ_c [−]: related to the strength of starch accumulation on photosynthesis (Eq (2))

- b_l^{max} [gFW]: maximum photosynthetically active leaf biomass (section 2.2)

- λ_{sdr}, λ_{sdi}, λ_{sni} [$\frac{1}{h}$]: parameters for γ dynamics (Eq (13))

- λ_g [−]: related to nightly starvation signal on growth (section 2.7)

- λ_f [$\frac{1}{h}$]: frequency parameter in nutrient consumption during photosynthesis (Eq (19) and (20))

- b_{r1}^{max} and b_{r2}^{max} [gFW]: maximum root biomass limiting uptake in each soil zone (section 2.6.1)

- λ_k [−]: coefficient related to the strength of stoichiometry signal in controlling uptake (Eq (29) and (30))

- b_r^c [gFW]: critical root biomass to reach subsoil zone from topsoil (section 2.4)

- λ_{sb} [$\frac{gFW}{\mu molC_6}$]: conversion parameter from sucrose to biomass (Eq (16), (17) and (18))

- λ_{csn} [−]: proportional parameter for c_{sn} (section 2.6)

In order to estimate them, we used the data available in [46]. In this work, the authors grew *Arabidopsis* under 5 different photoperiods ($4h$, $6h$, $8h$, $12h$, $18h$ of light) for 29 days assuming not limiting medium growth. Moreover, they measured sucrose and starch content and the aboveground rate of growth.

Within our model, we assumed only one soil zone ($b_r^c = +\infty$ and $n_{s2} = p_{s2} = 0\frac{\mu mol}{cm^3}$). Moreover, as already said, no competition effects were taken into account ($b_l^{max} = b_{r1}^{max} = b_{r2}^{max} = \infty$).

Of course, in estimating parameters we have to consider a strong dependence of natural processes by temperature. Since the influence of temperature was not explicitly modelled, we estimated different parameters for each photoperiod from [46], using a spline interpolation to approximate different day-lengths. For sake of simplicity, we tried to keep fixed the most of parameters. The best fitting was obtained assuming as variables only λ_c, λ_{sni}, λ_{sb}, obtaining the following values:

$$\lambda_c = [0.82\ 0.79\ 0.67\ 0.58\ 0.55]$$
$$\lambda_{sdr} = 0.25$$
$$\lambda_{sdi} = 0.1$$
$$\lambda_{sni} = [0.16\ 0.15\ 0.13\ 0.09\ 0.03]$$
$$\lambda_g = 0.65$$
$$\lambda_f = 0.066$$
$$\lambda_k = 50$$
$$\lambda_{sb} = [0.00345\ 0.00426\ 0.00527\ 0.00597\ 0.00646]$$
$$\lambda_{csn} = 0.0267$$

All experiments available to fit and validate the model are conducted in a vegetative phase and it was no possible to estimate a tissue death coefficient. Then, to avoid a greater number of free parameters, no explicit death is accounted in the model, even if the generalisation will be straightforward when new experiments will be available. However, a death concept can be considered present in the model by considering null the growth of the tissues (results for this consideration are reported in section 3.3).

3 Results

3.1 Model validation

We compared the results obtained by our model with the results extracted from the biological data available in [46].

We looked at the starch dynamic over different lengths of the day: 4, 6, 8, 12 and 18 ₃₀₃
hours (Fig 2A-C and Fig 3A-B). In each plot, red lines are piece-wise linear functions ₃₀₄
interpolating data from [46], while green lines are the numerical results obtained from ₃₀₅
our model. Blue dots represent the dawn (beginning of the day) and red ones the dusk ₃₀₆
(beginning of the night). The starch grows during the period of sunlight, and decrease ₃₀₇
during night with a good match between numerical and biological results. ₃₀₈

Fig 2. Validation test in short days.
Starch (from A to C) and sucrose (from D to F) dynamics for (A, D) 4h day length, (B,
E) 6h day length, (C, F) 8h day length. The red lines represent the data obtained
from [46], green lines are obtained from our numerical simulations. Blue dots are the
beginning of the day and red dots are the beginning of the night.

Fig 3. Validation test in long days.
Starch (in A and B) and sucrose (in C and D) dynamics for (A, C) 12h day length, (B,
D) 8h day length. The red lines represent the data obtained from [46], green lines are
obtained from our numerical simulations. Blue dots are the beginning of the day and
red dots are the beginning of the night.

The behaviour of the sucrose from numerical simulation (Fig 2D-F and Fig 3C-D) ₃₀₉
can be considered in average in agreement with biological data, even though less match ₃₁₀
is found between peaks of dawn and dusk. In fact, the oscillations in sucrose content are ₃₁₁
smoothed in the model. For instance, we can notice in 4h photoperiod (Fig 2D), instead ₃₁₂
of having two sucrose peaks during night, the model is able to simulate only one higher ₃₁₃
peak. A smoother behaviour is instead more evident in 18h of light (Fig 3D); a closer ₃₁₄
view on the oscillations for this photoperiod is reported in Fig 4A. Also in these plots, ₃₁₅
red lines fit experimental data, green lines represent simulations, while blue and red ₃₁₆
points are dawn and dusk respectively. Another defect concern the delay in the ₃₁₇
numerical results with respect to the experimental data. For instance in the 8h ₃₁₈
photoperiods (Fig 4B) there is a delay of 4h in the highest peak while in in the 18 ₃₁₉
photoperiods the delay is about of 6h. Anyway, the averaged dynamics well match ₃₂₀
simulation and biological results. ₃₂₁

Fig 4. Behaviour inaccuracies.
(A) Detail of sucrose content for 18h day length. (B) Detail of sucrose content for 8h
day length.

The reason for such delay can be imputed to the τ_{as} function, which formulation ₃₂₂
require more specific investigations (see file S1 in supporting information). Both the ₃₂₃
delay and the smoother dynamic effects could imply an on/off control on τ_{as}, with ₃₂₄
respect to some thresholds. Moreover, by assuming all parameters depending on ₃₂₅
photoperiods, it would be possible to further reduce the differences between model and ₃₂₆
biological data. However, we considered this validation sufficiently sharp (see next ₃₂₇
section 3.2), demonstrating the consistency of the model with respect to the literature. ₃₂₈
Finally, we compared the relative growth rates (RGR). In [46], the RGR of fresh
biomass of leaves is measured at the end of the night after 29 days. The mean values
extracted from the literature are reported in Table 1 and compared with the RGR
simulated by our model, obtaining an absolute error of $3.6283 \cdot 10^{-4}$. To compute the
RGR, we used the exponential formulation [73]:

$$RGR(t) = \frac{ln(gFW(t)) - ln(gFW(t_0))}{t - t_0} \tag{44}$$

where t_0 is the initial starting time. 329

Table 1. RGR obtained from literature and the model at different photoperiod.

Source	4h	6h	8h	12h	18h
[46]	0.068	0.1135	0.1708	0.26	0.3065
model	0.0682	0.1135	0.1707	0.2600	0.3064

330

331

3.2 Model robustness 332

To evaluate the robustness of our model, we compared the numerical results with data 333
extracted from several other papers. For instance, we tested the adaptation of the 334
model to different light periods. In [42], it is shown how plant changes its metabolism 335
and its sucrose content when day length changes from 8h to 16h (Fig 5).

Fig 5. Changing behaviour in [42].
Dynamic of sucrose content in sinks in *Arabidopsis* when passing from 8h to 16h of light
(in top left plot) and vice versa (in the top right plot). The black line refers to wild type
plants.

336

Since, we are not explicitly considering sucrose content in sinks, we simulated only 337
sucrose content dynamics passing from 8h light to 16h. The quantitative behaviour can 338
not be the same, but the qualitative behaviour is supposed to be consistent. In fact, our 339
model correctly predicts this dynamic as shown in Fig 6.

Fig 6. Changing behaviour in our model.
(A) Our model simulation of sucrose content when passing from 8h to 16h of light. (B)
Our model simulation of sucrose content when passing from 16h to 8h of light. Red line
is the simulation, while blue dots represent dark periods.

340

Just like in [42], in the day when photoperiod changes, plant adapts its behaviour in 341
an intermediate way, to fix it during successive days. 342
To verify the behaviour of γ we again referred to [42], in which γ varies along 343
different photoperiods and it is estimated according to Table 2.

Table 2. Values of γ at different photoperiods as extracted from [42]

	8h	9h	10h	11h	12h
γ	0.68	0.64	0.6	0.6	0.6

344

Nevertheless, [74] measured, in a standard experiment (12h of light), about 50% of 345
starch accumulation. More recently, [75] verified changes in starch accumulation 346
depending on photoperiod length and light intensity. The authors measured an 347
accumulation range of $[50\%, 68.7\%]$ for 6h photoperiods, and a range of $[36\%, 49.4\%]$ for 348
12h photoperiods. The more light intensity, the less starch stored. To verify these data 349
with our equations, we fixed non limiting initial conditions about nutrients and run the 350
model for 10 days. Table 3 reports the averaged values of γ, which result to be 351
consistent with data in the literature. 352
Another important validation is about the N:P ratio. In [23] it is shown how plant 353
tends fast to optimal ratio when a missing nutrient is inserted in the environment where 354
the roots grow. We fixed the value 10 according to the same reference and a light period 355

Table 3. Numerical results for γ at different photoperiods.

	6h	8h	9h	10h	11h	12h
γ	0.7	0.63	0.6	0.56	0.52	0.49

of 12h. To test this behaviour, we fixed soil conditions and we varied the initial nutrient ratio. Starting from a very small and an higher initial ratio, the behaviour tends to approach the optimal ratio (Fig 7).

Fig 7. Evolution of N:P at different initial conditions.
(A) N:P ratio in plant starting from a very little ratio (0.5); (B) N:P ratio in plant starting from the optimal situation; (C) N:P ratio in plant starting from a very large ratio (30).

Interestingly, [76] pointed out the role of N:P ratio in quantifying nutrient limitation on growth. Indeed, when we simulate different N and P soil contents, the plant reaches different stoichiometry ratios, as showed in Fig 8 (the point highlighted refers to N:P ratio in optimal nutrient soil content).

Fig 8. N:P dependence on soil nutrient contents

Moreover, when modelling the nutrient uptake, we assumed a dependence on the internal status instead of soil content. In [63], different values for both I_p^{max} and k_p were proposed for different plants of *Arabidopsis*. We averaged among them in order to estimate the hourly phosphorus content:

$$I_p^{max}\frac{p_s}{p_s + k_p},$$

in poor p soils ($p_s = 0.0025\frac{\mu molP}{cm^3}$) and rich p soils ($p_s = 0.5\frac{\mu molP}{cm^3}$). Then we run our model and computed hourly uptake:

$$I_p^{max}\frac{p_s}{p_s + k_p}a_p.$$

In Table 4 there is the comparison between numerical results and our model, for 16h of light and 7 days of growth, showing a maximum error of 3.52%.

Table 4. Hourly uptake of P for poor and rich p soil, obtained from literature and our model, with relative error.

Source	$p_s = 0.0025\frac{\mu molP}{cm^3}$	$p_s = 0.5\frac{\mu molP}{cm^3}$
[63]	0.108	0.142
Model	0.1075	0.147
Relative error (%)	0.46	3.52

Finally, we looked at the effects of excess and deficiency of P on growth. In [77] are reported two experiments on *Arabidopsis*, growing plants in 16h of light for 19 days under two different P treatments. The first treatment consists of a limited P medium ($p_s^L = 0.006 \frac{\mu mol P}{cm^3}$), and the second consists of a saturated P medium ($p_s^H = 1 \frac{\mu mol P}{cm^3}$). The authors measured the total dry biomass (DW) and the root:shoot ratio each 4 days. We used data from the 7th day as initial point and we compared both fresh biomass and root fraction at day 11th, 15th and 19th. Since our model is parametrized on fresh biomass, from [46] we estimated the relation DW$= 0.08FW$. Results, reported in Table 5, show an average error over the three periods of 0.028 ± 0.03 gDW in the rich soil and 0.00085 ± 0.00091 gDW in the poor soil, for the total biomass, and 0.43 ± 0.35 (%) in the rich soil and 1.71 ± 1.36 (%) in the poor soil, for the root fraction. The errors in biomass estimation, especially for the total biomass in rich soil, could be induced by the approximation adopted for FW to DW conversion. In fact, the water content could vary along the plant lifespan, affecting the relationship between dry and fresh weight.

Table 5. Total biomass and root:shoot biomass ratio obtained from literature and our model, with corresponding absolute error.

Source	Parameter	Treatment	11th day	15th day	19th day
[77]	Root fraction (%)	p_s^H	22.2	23.1	24.7
Model	Root fraction (%)	p_s^H	22.63	23.96	24.7
	Error		**0.43**	**0.86**	**0**
[77]	Root fraction (%)	p_s^L	49.4	50	54.6
Model	Root fraction (%)	p_s^L	45.96	51.59	54.7
	Error		**3.44**	**1.59**	**0.1**
[77]	total biomass (gDW)	p_s^H	0.01675	0.0398	0.057
Model	total biomass (gDW)	p_s^H	0.01874	0.04979	0.1299
	Error		**0.00199**	**0.00999**	**0.0729**
[77]	total biomass (gDW)	p_s^L	0.00287	0.00425	0.004875
Model	total biomass (gDW)	p_s^L	0.0025	0.0043	0.0070
	Error		**0.00037**	**0.00005**	**0.002125**

The evolution in time of the biomass and the root:shoot biomass ratio obtained from our numerical simulation is also reported in Fig 9.

Fig 9. Validation test on [77].
(A) Root percentage under high and low phosphorus treatments. (B) Biomass dynamics under high and low phosphorus treatments. In blue, simulations for saturated P, while in red simulations for limiting P.

3.3   Root behaviour in heterogeneous soils

Up to now, soil conditions were stationary in time and nutrients were supposed to be only in the topsoil zone. In this section, we arbitrary fix $b_r^c = 4 \cdot 10^{-5} gFW$ in order to study root system adaptation in heterogeneous soils. Results presented in the following refer to simulations of 20 days with 12h of light. We at first simulate root growth setting the topsoil rich in p, and the subsoil rich in n:

$$p_{s1} = 0.15 \frac{\mu mol P}{cm^3},$$
$$n_{s1} = 5 \frac{\mu mol N}{cm^3},$$
$$p_{s2} = 0 \frac{\mu mol P}{cm^3},$$
$$n_{s2} = 12 \frac{\mu mol N}{cm^3}.$$

From Fig 10A we can observe that no n is experienced in the subsoil zone (and consequently no root is allocated) until the critical mass is reached. Then, plant starts allocating resources to elongate in the subsoil zone. Of course, at the beginning the more P reduces the N:P ratio that is immediately increased when the subsoil is reached and the more nitrogen is available (Fig 10B).

Fig 10. Two soil zones effects.
(A) Root biomass growth in the two soil zones. Root growth in topsoil is drawn in blue line. Root growth in subsoil zone is drawn in red. (B) N:P ratio dynamics.

A more realistic simulation could be done assuming both nutrients initially placed in topsoil. But assuming that, day by day, nitrogen is transported by water from the topsoil to the subsoil:

$$p_{s1} = 0.15 \frac{\mu mol P}{cm^3},$$
$$n_{s1} = 12 \cdot 0.9^{i-1} \frac{\mu mol N}{cm^3},$$
$$p_{s2} = 0 \frac{\mu mol P}{cm^3},$$
$$n_{s2} = 12 - n_{s1} \frac{\mu mol N}{cm^3},$$

where the exponent i is the time (in days). Results are shown in Fig 11A. The less n_{s1} transported by water, the more n_{s2} accumulated in the subsoil.

Fig 11. Example of plant death.
(A) Root biomass growth in the two soil zones. Blue curve is the dynamic in the topsoil, red curve represents dynamics in subsoil. (B) Example of plant death. Blue line is the root growth in the topsoil, red line the root growth in the subsoil and green line is the aboveground growth.

To simulate a deeper nitrogen leak and then an higher topsoil zone missing n, the critical biomass b_r^c can be increased. Moreover, it can happen the death of the plant, if nitrogen is lost faster than the time needed by roots for soil exploration. This condition

can be obtained by the absence of growth. Let's assume:

$$p_{s1} = 0.15 \frac{\mu mol P}{cm^3},$$

$$n_{s1} = 12 \cdot 0.3^{i-1} \frac{\mu mol N}{cm^3},$$

$$p_{s2} = 0 \frac{\mu mol P}{cm^3},$$

$$n_{s2} = 12 - n_{s1} \frac{\mu mol N}{cm^3},$$

$$b_r^c = 9 \cdot 10^{-5}.$$

In this case, the root biomass is not able to grow up enough to reach the subsoil, although the greater investment in roots (different slopes in blue and green curves in Fig 11B). This way, the nitrogen is quickly exhausted and the plant is not able to survive.

We also verified the adaptive behaviour of plant in rich-soil zones (as reviewed in [55]):

$$p_{s1} = 0.09 \cdot 0.6^{i-1} \frac{\mu mol P}{cm^3}$$

$$n_{s1} = 7.2 \cdot 0.9^{i-1} \frac{\mu mol N}{cm^3}$$

$$p_{s2} = 0.15 \frac{\mu mol P}{cm^3}$$

$$n_{s2} = 12 \frac{\mu mol N}{cm^3}$$

$$b_r^c = 5 \cdot 10^{-6}$$

The plant used to grow in a more and more limiting topsoil, until the subsoil is reached. The more nutrient availability stimulates the growth in the deeper soil zone (Fig 12A).

Fig 12. Changing soil zones.
(A) Example of adaptation to different soil nutrient patches. The green line describes leaves, blue and red curve represent topsoil and subsoil roots respectively. (B) Example of N:P adaptation to different soil nutrient patches. (C) Example of the evolution of root fraction (green line) and root priority (f_r) (magenta line) in adaptation to different soil nutrient patches. (D) Example of uptake adaptation to different soil nutrient patches.

Actually, the behaviour is more complex than what Fig 12A can express and the plant is, indeed, able to compute different signals at the same time. To show how our model simulate this complex network of stimuli, we provide additional results in the same framework of the previous simulation. Fig 12B shows the dynamics of N:P stoichiometry ratio and Fig 12C shows the evolution of root fraction and root priority (f_r).

The adaptation of uptake signals a_n (magenta line for nitrogen) and a_p (light blue line for phosphorus) is instead presented in Fig 12D. In the end, the balance between uptake gain (u_n and u_p) and nitrogen and phosphorus costs (C_n and C_p) are shown in Fig 13.

Fig 13. Example of adaptation to different soil nutrient patches. The blue dots represent nitrogen balance ($\frac{u_n}{u_n+C_n}$), while the red dots the phosphorus one ($\frac{u_p}{u_p+C_p}$).

All together, these plots allow us to appreciate a deeper simulation of plant 404
adaptation. In fact, at the beginning, the plant experiences both low n and p in the 405
topsoil. The limiting resources promote a greater uptake and a greater root priority. In 406
Fig 12C the root fraction quickly increases. Moreover, the phosphorus is more limiting 407
than nitrogen. In fact, in Fig 13 the averaged nitrogen balance is higher than the 408
averaged phosphorus balance (the difference is evident at the beginning of the graph). 409
This leads to a greater N:P ratio (Fig 12B) and a smaller a_n. 410

However, according to [55], differences in uptake costs and root growth costs define 411
the nutrient affinity improvement of plant or the increasing of root fraction. In the 412
phosphorus limiting case, being the soil exploration useless due to nutrient deficiency 413
(until the subsoil is reached), it is more convenient to increase phosphorus affinity a_p 414
more than root fraction (light blue curve in Fig 12D and magenta curve in Fig 12C). On 415
the other hand, when the rich soil is reached, plant cannot immediately change its 416
strategies due to the concept of memory [18]. In fact, plots show no changes in 417
dynamics after having passed the topsoil boundary. Anyway, more phosphorus is now 418
available and the unmodified strategy leads to luxury uptake of phosphorus and a 419
critical reduced N:P ratio (Fig 12B). To stabilise the stoichiometry ratio, plant starts 420
reducing phosphorus affinity. Moreover, in rich soil zones, the uptake is more convenient 421
than root proliferation, so that root priority is less strong than a_n. In the end, when 422
both the optimal ratio is reached and the memory is coordinated with the new soil 423
nutrient content, plant can stabilise its signals. 424

3.4   Leaf-root competition 425

We simulate leaf and root competition by fixing parameters b_l^{max}, b_{r1}^{max} and b_{r2}^{max}. For 426
this analysis, we assumed only one soil zone with optimal nutrient contents and we 427
performed a simulation of 20 days. When assuming $b_l^{max} = 0.3gFW$, the critical leaf 428
biomass is reached after $t = 343h$. However, even after the critical biomass, plant does 429
not stop growing (Fig 14)but the sucrose is not enough to sustain the actual growth 430
(Fig 15A). This is the signal that later will reduce the growth. Both leaves and roots 431
decrease with respect to a plant not experiencing the competition (Fig 15B and 15C). 432
Of course, there are no reasons why affinity should change (for example in Fig 15E we 433
report the phosphorus affinity a_p being similar also the a_n dynamics). Letting 434
conditions unchanged and simulating 50 days, a new equilibrium is reached by the plant 435
(Fig 15E).

Fig 14. Effects of leaf competition on plant biomass. (A) Total behaviour. (B) Detail close to $= t324.4h$. In blue the case of no competition, while in red the case of $b_l^{max} = 0.3gFW$.

Fig 15. Effects of leaf competition on plant biomass. In blue the case of no competition, while in red the case of $b_l^{max} = 0.3gFW$.
(A) Sucrose dynamics (B) Leaf dynamics (C) Root dynamics (D) Sucrose dynamics for a dynamic of 50 days showing a new stabilisation (E) Adaptation of phosphorus uptake feedback (being the nitrogen one similar)

436

3.5 Root overproduction

According to [78] and [79], the competition among adjacent roots occurs when the respective rhizosphere overlaps the other one, reducing the uptake for unit of root mass. This is consistent with our modelling approach (see section 2.6.1). For this evaluation, we assumed only one soil zone, $b_{r1}^{max} = 0.3gFW$ and, initially, no leaf competition. We performed simulations for 20 days at 12h of light, and the results are shown in Fig 16. As expected, plant promotes leaf growth instead of the root one.

Fig 16. Effects of root competition on roots and leaves.
The blue curve is growing without competition.

However, for a more realistic framework we should take into account also leaf competition. For this reason, we further simulate the behaviour in two conditions: $b_l^{max} = 2.3gFW$ and $b_l^{max} = 1gFW$.
In the former case (greater leaf critical biomass), the strategy is dangerous because favouring leaves than roots, roots can not absorb enough nutrients to sustain the faster leaf growth. At the beginning, the total biomass is greater with respect to the no competition framework (red curve in Fig 17A).

Fig 17. Total competition effects.
(A) Effects of later leaf competition and faster root competition on plant biomass. (B) Effects of plant death due to a later leaf competition. (C) Effects of faster leaf and root competition in plant biomass.

After few days (25 instead of 20 days) the plant dies (red curve in Fig 17B). In the second case, the leaf competition happens when the plant can still sustain its development. The growth still hold but in a slower way and the plant does not die (red curve in Fig 17C).
Finally, let's assume two optimal soil zones ($b_r^c = 0.1gFW$) in a competing framework ($b_l^{max} = 0.3gFW$ and $b_{r1}^{max} = 0.05gFW$) for 30 days. Initially, the plant experiences the competition inducing an unbalance between nutrients: the N:P ratio is not anymore optimal (Fig 18A). After having reached the subsoil, the plant promotes the root growth in the subsoil (Fig 18B and 18C) and stabilises again the optimal ratio.

Fig 18. Effects of leaf and root competition in two soil zones.
(A) N:P ratio. (B) Subsoil roots vs topsoil roots. (C) Root to shoot ratio.

4 Discussions

In this paper, we took stock of existing biological literature extrapolating the main evidences of intra-plant communication in the form of interactions between the dynamics of internal processes in plants. By the experimental data obtained from literature, it was possible to point out the relationships between such processes and to define realistic parameters for the equations proposed in the model.
To date, the mathematical models of plant growth actually disregard plant communication. They mainly focus on the description of a single and specific process such as photosynthesis, uptake or water transport; they are devoted to the description of the chemical interaction among hormones; or limited to a single nutrient.
To have a glance on the internal communication driving the growth, and differently from the state of the art, we proposed here a model that integrates at the same time

several processes (photosynthesis, starch degradation, nutrients uptake and   472
management, biomass allocation, maintenance), different signals (circadian clock and   473
growth stimulus) and nutrients (sucrose, nitrogen and phosphorus).   474

The overall system extends results from previous models ([20, 41]) and proposes an   475
approach, that could be addressed to biologists, for analysing interactions not yet   476
investigated. For example, thanks to the model it is possible to evaluate how   477
photosynthesis intensity and sucrose production rate are reduced or increased according   478
to different stoichiometry ratio values, or which process is mainly, and earlier, affected   479
by nightly starvation. By evaluating the dynamics of the priority signal f_r when the   480
environmental conditions change, it is possible to investigate on the effects of starch   481
accumulation during biomass allocation. Furthermore, one may inquire responses to   482
leaves and roots overproduction or photosynthesis limitations due to light and stored   483
starch.   484

Also, new questions about the nutrient uptake mechanism emerged from the model.   485
In fact, the classic Michaelis-Menten dynamics ([63–65]) was generalised to include   486
internal stimuli. The accuracy of results suggests the need for new biological   487
experiments to additionally investigate on this mechanism.   488

Comparing our model with [20, 42], a new relation has been defined for the growth,   489
which does not depend anymore just on nutrients availability, but it takes into account   490
also starvation and efficiency. Here, by efficiency of an organ (which could be a leaf or a   491
root), we mean the ability of that organ to provide the amount of resources needed for   492
the correct functioning and growth. For example, the roots efficiency is the ability to   493
provide both nitrogen and phosphorus such that nutrient levels are enough to sustain   494
hourly costs of nitrogen (C_n) and phosphorus (C_p). On the other hand, leaves efficiency   495
is the ability to produce enough sucrose and starch so that all respiration costs (r_m, r_m^u,   496
r_m^t, r_g) are covered by the available sucrose. Hence, as reviewed in this paper, plant   497
tries to never reach minimum nutrients thresholds, while keeping monitored level of   498
stores to avoid consuming energy unnecessarily.   499

What the model can show, by analysing these dynamics, is a dense network of   500
signals and feedback that enforce the concept of intra-plant communication allowing a   501
deeper understanding of how this internal network is connected.   502

Nevertheless, the model can be used to better define biological concepts like   503
performance, nutrient *efficiency* and *sink priority*.   504

In [24], *performance* is defined as *"the ability to acquire resources and survive in the*   505
presence of competition or in stressful environments where physiological limits are   506
reached". The problem in measuring the performance refers to the problem of defining   507
the parameter to be checked in stressful conditions: either the biomass, sucrose   508
production, nutrient uptake or photosynthate allocation are important parameters that   509
can provide an idea about the ability of the plant to survive. Our model allows to easily   510
estimate the plant performance by simulating limiting scenarios and measuring sucrose,   511
nitrogen and phosphorus levels with respect to the critical thresholds.   512

In [80], the *efficiency* in using nutrients is generally defined as: the *"measure of how*   513
well plants use the available mineral nutrients. It can be defined as yield (biomass) per   514
unit input (fertiliser, nutrient content)". A similar definition can be found in [25] for   515
efficiency in the use of water, and related to photosynthesis efficiency.   516

Clearly, the biomass parameter is not enough to measure the efficient use of nutrient;   517
in fact, just considering this parameter, a simple imbalance in roots and leaves biomass   518
could imply a not efficient use of resources, whereas it is not always the case [81]. In our   519
model, the efficiency emerges from relationships among uptake and nutrient costs (from   520
Eq (29) and (30)). In fact, it is possible to note a nutrient efficiency in the first ratio,   521
relating uptake (u_n and u_p) with costs (C_n and C_p), and a photosynthesis efficiency in   522
the last ratio, which relates uptake and photosynthesis. In addition, Eq (13), relating   523

sucrose and its critical thresholds, gives an idea about sucrose efficiency. $_{524}$

Finally, [82] defines the strength of sinks, or *sink priority*, as *"the competitive ability* $_{525}$ *of a sink organ to import photoassimilates, and depends on both its physical (size) and* $_{526}$ *physiological (activity) capabilities"*. While the size is a clear parameter and it can be $_{527}$ easily related to the biomass of the organ, defining the activity of a sink is more $_{528}$ difficult. In [83], the term *sink activity* is referred to all processes involved in using $_{529}$ resources, from the synthesis of new tissues to the maintenance of the already existing $_{530}$ ones. This activity can be quantified as the net assimilation of resources in tissues $_{531}$ minus losses due to respiration and exudation. However, in [84] it is noted how the $_{532}$ previous definition of sink strength is not enough to explain how sucrose is allocated in $_{533}$ the plant. In fact, processes affecting osmotic concentrations in sinks need to be taken $_{534}$ into account for resources allocation. Furthermore, in [83], is highlighted the importance $_{535}$ of associating the source-sink interaction with the whole plant growth, even if no hint $_{536}$ about how to do it is given. $_{537}$

In our model, both the sucrose partitioning signal (f_r) and the root competition $_{538}$ function (e_1) are used to describe this *sink priority*. They depend on resources content $_{539}$ (taking into account osmotic concentration) and, indirectly, on the biomass (size) and $_{540}$ internal processes (activity). In this way, it is possible to connect the general definition $_{541}$ of sink strength with the concept of osmotic concentration, other than proposing a $_{542}$ practical association between plant growth and source-sink interactions, through the $_{543}$ effects of f_r and e_1 on the biomass dynamics (leaves b_l and roots b_r). $_{544}$

5   Conclusions $_{545}$

Plants are an important model of adaptation by acting with morphological and $_{546}$ physiological responses to environmental changes. The richness in internal and external $_{547}$ signals that plants use for regulating their growth strategies are opening new frontiers $_{548}$ about the ability of plant to communicate ([1]). The understanding of the processes $_{549}$ and actors behind their communication is of fundamental importance not only for $_{550}$ improving the knowledge of plant functioning, but also for helping in translating such $_{551}$ abilities in many other fields for different applications (e.g. for collaborative tasks in $_{552}$ swarm robotics [23], for resolution of combinatorial problems [85]). $_{553}$

The mechanisms of plant communication are being studied through self-recognition $_{554}$ cues, underground interactions with fungi or other plants, volatile organic compounds, $_{555}$ electric and chemical signals ([86–88]). In this paper, we investigated in the intra-plant $_{556}$ communication by analysing the possible cues activating the adaptive growth responses $_{557}$ in a single plant and describing the dynamics of such internal processes and signals with $_{558}$ a mathematical model. Our assumptions and formulations have been deeply analysed in $_{559}$ comparison with other models from the state of the art, highlighting the adopted $_{560}$ extensions and improved potentialities. $_{561}$

Main difference with other models is having included several different elements (e.g. $_{562}$ photosynthesis, starch degradation, multiple nutrients uptake and management, biomass $_{563}$ allocation, maintenance) and their dynamics all at once considering their interactions $_{564}$ and effects on the growth, thus showing the potential intra-communication in plants; $_{565}$ whereas, strength of our model lies in having based assumptions and formulations on $_{566}$ biological evidences and laboratory experiments collected from the state of the art. This $_{567}$ approach allowed to evaluate several parameters from the papers thus reducing the $_{568}$ number of free variables, and at the same time, to maintain a high level of details with $_{569}$ good agreements with the biological model. $_{570}$

To test the robustness of our model, we compared the biomass, sucrose dynamics, $_{571}$ photosynthesis partitioning rate, uptake strength and sinks priorities not using custom $_{572}$ experiments, but encouraging the comparison with different independent published $_{573}$

biological data. Indeed, we validated the model by comparing experimental results with $\quad$ 574
results obtained in our simulations, reproducing conditions of growth similar to the $\quad$ 575
biological counterpart. All validation tests show high accuracy in results and very small $\quad$ 576
errors (e.g., we obtained 3.52% as maximum relative error in nutrient uptake $\quad$ 577
comparisons (Table 4) and 3.44% as maximum percentage error for biomass estimation $\quad$ 578
in low phosphorus soil tests (Table 5)); where, the errors obtained are likely induced by $\quad$ 579
divergences of initial conditions between biological and numerical experiments. However, $\quad$ 580
both the qualitative behaviour and the quantitative values agree with data in literature. $\quad$ 581

Moreover, we simulated different growth scenarios. Interestingly, in stress conditions, $\quad$ 582
e.g. when the saturating thresholds were reached, the dynamics showed a fast $\quad$ 583
adaptation of the plant with a self-optimisation of internal resources and feedback $\quad$ 584
stimuli, without the need of a *a-priori* optimisation assumption. The same self-adaptive $\quad$ 585
behaviour was evident when branching vs elongation was analysed. This optimising $\quad$ 586
behaviour is realistic but difficult to be biologically demonstrated. However, differently $\quad$ 587
to some models [4, 19] that directly start by assuming the existence of an internal $\quad$ 588
optimisation function which drives plant dynamics, in here we demonstrated it to be a $\quad$ 589
consequently behaviour emerging from the dynamics of internal processes. Therefore, $\quad$ 590
our model enforces the idea of an emerging behaviour in plants making use of an $\quad$ 591
internal communication network for optimising the use of the internal resources, the $\quad$ 592
exploration of the soil and the adaptation of internal processes, and results in an $\quad$ 593
efficient growth strategy [23]. $\quad$ 594

Beside important biological implications and analysis, this model can also leverage $\quad$ 595
the development of plant-inspired algorithms for the control of exploratory robots $\quad$ 596
([89], [23]). For instance, the equations, identically replicated on each robot, can $\quad$ 597
describe the behaviour of the robot and represent the ability of robotic roots to colonise $\quad$ 598
a certain area (plant branching) or to growth further in exploration (plant elongation), $\quad$ 599
according to the internal signals (into the colony of robots) and the measurements from $\quad$ 600
the environment. $\quad$ 601

Future steps will include from one side, the implementation of the proposed $\quad$ 602
behaviour in robotic solutions, while from a biological perspective several improvements $\quad$ 603
can be adopted. For instance, the saturating thresholds can be replaced by death terms $\quad$ 604
that need to be estimated via laboratory experiments. Stem and fruit dynamics can be $\quad$ 605
introduced for a more complete description. Moreover, the concepts for resources $\quad$ 606
allocation, analysed in this paper only in roots, could be used to study resources $\quad$ 607
partitioning in leaves. Additionally, from a mathematical point of view, partial $\quad$ 608
differential equations can replace root dynamics to analyse spatial diffusion of roots. $\quad$ 609
Moreover, the model is easily embeddable with more detailed formulations for $\quad$ 610
photosynthesis, light, temperature, starch degradation, respiration or exudation in order $\quad$ 611
to make the model more and more detailed. $\quad$ 612

Ultimately, the model can become a powerful tool for the study and validation of $\quad$ 613
biological hypothesis; step by step introducing additional dynamics, it can describe $\quad$ 614
complex behaviours and help in finding the signals driving them; it can further be $\quad$ 615
integrated for study the interactions among two or more plants or for instance, to $\quad$ 616
highlight the effects of having invasive or not-invasive species. If coupled with nutrients $\quad$ 617
dynamics in soil, the model can provide useful tools for optimising outer resources $\quad$ 618
distribution to reach a target biomass. As well as, a coupling with a stochastic model of $\quad$ 619
temperature and light can allow a study of a seasonal adaptation of the plant. $\quad$ 620

6   Supporting information $\quad$ 621

S1 Appendix.   Starch degradation comparison. A more detailed starch $\quad$ 622
degradation function is integrated in the model. The results are discussed and new open $\quad$ 623

questions are proposed about this complex chemical process.   624

References

1. Karban R. Plant behaviour and communication. Ecology letters. 2008;11(7):727–739.

2. Arber A. The natural philosophy of plant form. Cambridge University Press; 2012.

3. Silvertown J, Gordon DM. A framework for plant behavior. Annual Review of Ecology and Systematics. 1989;20(1):349–366.

4. Trewavas A. What is plant behaviour? Plant, cell & environment. 2009;32(6):606–616.

5. Chew YH, Smith RW, Jones HJ, Seaton DD, Grima R, Halliday KJ. Mathematical models light up plant signaling. The Plant Cell. 2014; p. tpc–113.

6. Gallé A, Lautner S, Flexas J, Fromm J. Environmental stimuli and physiological responses: the current view on electrical signalling. Environmental and Experimental Botany. 2015;114:15–21.

7. Hedrich R, Salvador-Recatalà V, Dreyer I. Electrical wiring and long-distance plant communication. Trends in Plant Science. 2016;21(5):376–387.

8. Barak S, Tobin EM, Green RM, Andronis C, Sugano S. All in good time: the Arabidopsis circadian clock. Trends in plant science. 2000;5(12):517–522.

9. Dodd AN, Belbin FE, Frank A, Webb AA. Interactions between circadian clocks and photosynthesis for the temporal and spatial coordination of metabolism. Frontiers in plant science. 2015;6:245.

10. Grigolon S, Bravi B, Martin OC. Responses to auxin signals: an operating principle for dynamical sensitivity yet high resilience. Royal Society open science. 2018;5(1):172098.

11. Muraro D, Byrne H, King J, Bennett M. The role of auxin and cytokinin signalling in specifying the root architecture of Arabidopsis thaliana. Journal of theoretical biology. 2013;317:71–86.

12. Allen HR, Ptashnyk M. Mathematical modelling and analysis of the brassinosteroid and gibberellin signalling pathways and their interactions. Journal of theoretical biology. 2017;432:109–131.

13. Javaux M, Couvreur V, Vanderborght J, Vereecken H. Root water uptake: From three-dimensional biophysical processes to macroscopic modeling approaches. Vadose Zone Journal. 2013;12(4).

14. Vogel T, Votrubova J, Dohnal M, Dusek J. A simple representation of plant water storage effects in coupled soil water flow and transpiration stream modeling. Vadose Zone Journal. 2017;16(5).

15. Minchin PE, Lacointe A. Consequences of phloem pathway unloading/reloading on equilibrium flows between source and sink: a modelling approach. Functional plant biology. 2017;44(5):507–514.

16. Jensen KH, Berg-Sørensen K, Bruus H, Holbrook NM, Liesche J, Schulz A, et al. Sap flow and sugar transport in plants. Reviews of modern physics. 2016;88(3):035007.

17. Franklin O, Cambui CA, Gruffman L, Palmroth S, Oren R, Näsholm T. The carbon bonus of organic nitrogen enhances nitrogen use efficiency of plants. Plant, cell & environment. 2017;40(1):25–35.

18. Xu C, Fisher R, Wullschleger SD, Wilson CJ, Cai M, McDowell NG. Toward a mechanistic modeling of nitrogen limitation on vegetation dynamics. PloS one. 2012;7(5):e37914.

19. Manoli G, Bonetti S, Domec JC, Putti M, Katul G, Marani M. Tree root systems competing for soil moisture in a 3D soil–plant model. Advances in water resources. 2014;66:32–42.

20. Feller C, Favre P, Janka A, Zeeman SC, Gabriel JP, Reinhardt D. Mathematical modeling of the dynamics of shoot-root interactions and resource partitioning in plant growth. PloS one. 2015;10(7):e0127905.

21. Manoli G, Huang CW, Bonetti S, Domec JC, Marani M, Katul G. Competition for light and water in a coupled soil-plant system. Advances in Water Resources. 2017;108:216–230.

22. Méndez V, Campos D, Sheppard AW. A model for plant invasions: the role of distributed generation times. Bulletin of mathematical biology. 2009;71(7):1727–1744.

23. Del Dottore E, Mondini A, Sadeghi A, Mazzolai B. Swarming Behavior Emerging from the Uptake–Kinetics Feedback Control in a Plant-Root-Inspired Robot. Applied Sciences. 2018;8(1):47.

24. Younginger BS, Sirová D, Cruzan MB, Ballhorn DJ. Is biomass a reliable estimate of plant fitness? Applications in plant sciences. 2017;5(2):1600094.

25. Hopmans JW, Bristow KL. Current capabilities and future needs of root water and nutrient uptake modeling. In: Advances in agronomy. vol. 77. Elsevier; 2002. p. 103–183.

26. Barker AV, Pilbeam DJ. Handbook of plant nutrition. CRC press; 2015.

27. Hopkins WG, Hüner N. Introduction to plant physiology. 581.1 H6 2004; 2004.

28. Malagoli P, Le Deunff E. An updated model for nitrate uptake modelling in plants. II. Assessment of active root involvement in nitrate uptake based on integrated root system age: measured versus modelled outputs. Annals of botany. 2014;113(6):1007–1019.

29. Meunier F, Draye X, Vanderborght J, Javaux M, Couvreur V. A hybrid analytical-numerical method for solving water flow equations in root hydraulic architectures. Applied Mathematical Modelling. 2017;52:648–663.

30. Roose T, Fowler A, Darrah P. A mathematical model of plant nutrient uptake. Journal of mathematical biology. 2001;42(4):347–360.

31. Leghari SJ, Wahocho NA, Laghari GM, HafeezLaghari A, MustafaBhabhan G, HussainTalpur K, et al. Role of nitrogen for plant growth and development: A review. Advances in Environmental Biology. 2016;10(9):209–219.

32. Roy R, Finck A, Blair G, Tandon H. Plant nutrition for food security. A guide for integrated nutrient management FAO Fertilizer and Plant Nutrition Bulletin. 2006;16:368.
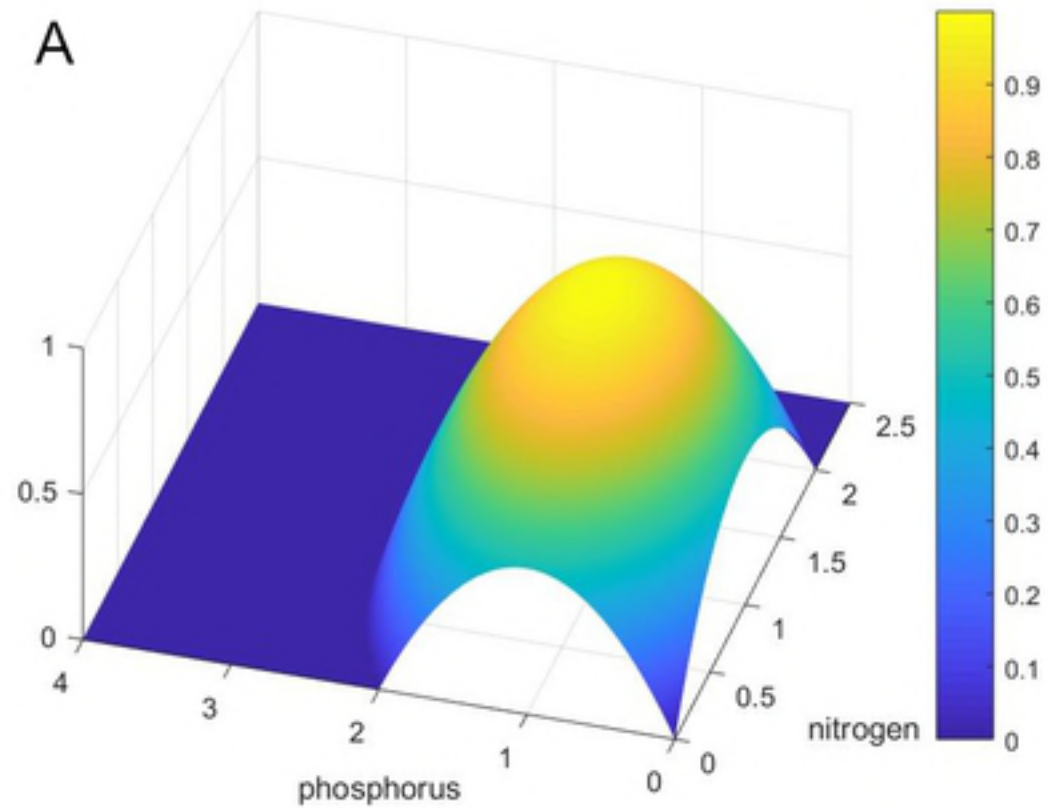
33. Buckley TN. Modeling stomatal conductance. Plant physiology. 2017;174(2):572–582.

34. Goldschmidt EE, Huber SC. Regulation of photosynthesis by end-product accumulation in leaves of plants storing starch, sucrose, and hexose sugars. Plant physiology. 1992;99(4):1443–1448.

35. Stitt M. Rising CO2 levels and their potential significance for carbon flow in photosynthetic cells. Plant, Cell & Environment. 1991;14(8):741–762.

36. Feugier FG, Satake A. Dynamical feedback between circadian clock and sucrose availability explains adaptive response of starch metabolism to various photoperiods. Frontiers in plant science. 2013;3:305.

37. Evans JR. Photosynthesis and nitrogen relationships in leaves of C 3 plants. Oecologia. 1989;78(1):9–19.

38. Arnon DI. Phosphorus metabolism and photosynthesis. Annual Review of Plant Physiology. 1956;7(1):325–356.

39. Browne CA. Liebig and the law of the minimum. Liebig and after Liebig Publication. 1942;(16):71–82.

40. Smith AM, Stitt M. Coordination of carbon supply and plant growth. Plant, cell & environment. 2007;30(9):1126–1149.

41. Seki M, Ohara T, Hearn TJ, Frank A, Silva VC, Caldana C, et al. Adjustment of the Arabidopsis circadian oscillator by sugar signalling dictates the regulation of starch metabolism. Scientific Reports. 2017;7(1):8305.

42. Ohara T, Satake A. Photosynthetic entrainment of the circadian clock facilitates plant growth under environmental fluctuations: perspectives from an integrated model of phase oscillator and phloem transportation. Frontiers in plant science. 2017;8:1859.

43. Feugier FG, Satake A. Hyperbolic features of the circadian clock oscillations can explain linearity in leaf starch dynamics and adaptation of plants to diverse light and dark cycles. Ecological modelling. 2014;290:110–120.

44. Haydon MJ, Mielczarek O, Robertson FC, Hubbard KE, Webb AA. Photosynthetic entrainment of the Arabidopsis thaliana circadian clock. Nature. 2013;502(7473):689.

45. Paparelli E, Parlanti S, Gonzali S, Novi G, Mariotti L, Ceccarelli N, et al. Nighttime sugar starvation orchestrates gibberellin biosynthesis and plant growth in Arabidopsis. The plant cell. 2013; p. tpc–113.

46. Sulpice R, Flis A, Ivakov AA, Apelt F, Krohn N, Encke B, et al. Arabidopsis coordinates the diurnal regulation of carbon allocation and growth across a wide range of photoperiods. Molecular Plant. 2014;7(1):137–155.

47. Martins MCM, Hejazi M, Fettke J, Steup M, Feil R, Krause U, et al. Feedback inhibition of starch degradation in Arabidopsis leaves mediated by trehalose 6-phosphate. Plant physiology. 2013; p. pp–113.

48. Truernit E. Plant physiology: the importance of sucrose transporters. Current Biology. 2001;11(5):R169–R171.

49. Jensen KH, Liesche J, Bohr T, Schulz A. Universality of phloem transport in seed plants. Plant, cell & environment. 2012;35(6):1065–1076.

50. Lacointe A, Minchin PE. Modelling phloem and xylem transport within a complex architecture. Functional Plant Biology. 2008;35(10):772–780.

51. Hermans C, Hammond JP, White PJ, Verbruggen N. How do plants respond to nutrient shortage by biomass allocation? Trends in plant science. 2006;11(12):610–617.

52. Harpole WS, Ngai JT, Cleland EE, Seabloom EW, Borer ET, Bracken ME, et al. Nutrient co-limitation of primary producer communities. Ecology letters. 2011;14(9):852–862.

53. Poorter H, Nagel O. The role of biomass allocation in the growth response of plants to different levels of light, CO2, nutrients and water: a quantitative review. Functional Plant Biology. 2000;27(12):1191–1191.

54. Poorter H, Niklas KJ, Reich PB, Oleksyn J, Poot P, Mommer L. Biomass allocation to leaves, stems and roots: meta-analyses of interspecific variation and environmental control. New Phytologist. 2012;193(1):30–50.

55. Hodge A. The plastic plant: root responses to heterogeneous supplies of nutrients. New phytologist. 2004;162(1):9–24.

56. Liu Y, Bortier MF, De Boeck HJ, Nijs I. Root distribution responses to three-dimensional soil heterogeneity in experimental mesocosms. Plant and soil. 2017;421(1-2):353–366.

57. Wang Y, Zhang Y. Soil-phosphorus distribution and availability as affected by greenhouse subsurface irrigation. Journal of Plant Nutrition and Soil Science. 2010;173(3):345–352.

58. Tinker PB, Nye PH. Solute movement in the rhizosphere. Oxford University Press; 2000.

59. Morris EC, Griffiths M, Golebiowska A, Mairhofer S, Burr-Hersey J, Goh T, et al. Shaping 3D root system architecture. Current Biology. 2017;27(17):R919–R930.

60. Pons T, Lambers H, Chapin III F. Plant physiological ecology; 1998.

61. Epstein E. Mineral nutrition of plants; principles and perspective; 1972.

62. Kung SD, Yang SF. Discoveries in plant biology. vol. 3. World scientific; 2000.

63. Narang RA, Bruene A, Altmann T. Analysis of phosphate acquisition efficiency in different Arabidopsis accessions. Plant Physiology. 2000;124(4):1786–1799.

64. Jungk A, Asher C, Edwards D, Meyer D. Influence of phosphate status on phosphate uptake kinetics of maize (Zea mays) and soybean (Glycine max). In: Plant Nutrition—Physiology and Applications. Springer; 1990. p. 135–142.

65. Siddiqi MY, Glass AD, Ruth TJ, Rufty TW. Studies of the uptake of nitrate in barley: I. Kinetics of 13NO3- influx. Plant Physiology. 1990;93(4):1426–1432.

66. Marin E, Thibaud MC, Paul-lez Durance Cedex F. Measurement of 33P-PO4 Absorption Kinetic Constants in Arabidopsis. Plant Physiology. 2015;.

67. Kotur Z, Siddiqi YM, Glass AD. Characterization of nitrite uptake in Arabidopsis thaliana: evidence for a nitrite-specific transporter. New Phytologist. 2013;200(1):201–210.

68. Yan Z, Guan H, Han W, Han T, Guo Y, Fang J. Reproductive organ and young tissues show constrained elemental composition in Arabidopsis thaliana. Annals of botany. 2016;117(3):431–439.

69. Herms DA, Mattson WJ. The dilemma of plants: to grow or defend. The quarterly review of biology. 1992;67(3):283–335.

70. de Groot CC, Marcelis LF, van den Boogaard R, Kaiser WM, Lambers H. Interaction of nitrogen and phosphorus nutrition in determining growth. Plant and Soil. 2003;248(1-2):257–268.

71. Fageria V. Nutrient interactions in crop plants. Journal of plant nutrition. 2001;24(8):1269–1290.

72. Moseley JL, Allinger T, Herzog S, Hoerth P, Wehinger E, Merchant S, et al. Adaptation to Fe-deficiency requires remodeling of the photosynthetic apparatus. The EMBO Journal. 2002;21(24):6709–6720.

73. Hoffmann WA, Poorter H. Avoiding bias in calculations of relative growth rate. Annals of botany. 2002;90(1):37–42.

74. Smith AM, Zeeman SC, Smith SM. Starch degradation. Annu Rev Plant Biol. 2005;56:73–98.

75. Mengin V, Pyl ET, Alexandre Moraes T, Sulpice R, Krohn N, Encke B, et al. Photosynthate partitioning to starch in Arabidopsis thaliana is insensitive to light intensity but sensitive to photoperiod due to a restriction on growth in the light in short photoperiods. Plant, cell & environment. 2017;40(11):2608–2627.

76. Güsewell S. N: P ratios in terrestrial plants: variation and functional significance. New phytologist. 2004;164(2):243–266.

77. Trull M, Guiltinan M, Lynch J, Deikman J. The responses of wild-type and ABA mutant Arabidopsis thaliana plants to phosphorus starvation. Plant, Cell & Environment. 1997;20(1):85–92.

78. Ge Z, Rubio G, Lynch JP. The importance of root gravitropism for inter-root competition and phosphorus acquisition efficiency: results from a geometric simulation model. Plant and Soil. 2000;218(1-2):159–171.

79. Rubio G, Walk T, Ge Z, Yan X, Liao H, Lynch JP. Root gravitropism and below-ground competition among neighbouring plants: a modelling approach. Annals of Botany. 2001;88(5):929–940.

80. Meena VS, Verma JP, Meena SK. Nutrient Use Efficiency in Plants: Concepts and Approaches, Malcolm J. Hawkesford, Stanislav Kopriva, Luit J. De Kok (Eds.). Springer (2014), 279 pp., Price€ 118.99, ISBN: 978-3-319-10634-2 (Print) 978-3-319-10635-9 (Online); 2015.

81. Hodge A. Root decisions. Plant, Cell & Environment. 2009;32(6):628–640.

82. Bihmidine S, Hunter III CT, Johns CE, Koch KE, Braun DM. Regulation of assimilate import into sink organs: update on molecular drivers of sink strength. Frontiers in Plant Science. 2013;4:177.

83. White AC, Rogers A, Rees M, Osborne CP. How can we make plants grow faster? A source–sink perspective on growth rate. Journal of Experimental Botany. 2015;67(1):31–45.

84. Evans LT, Wardlaw IF. Wheat. In: Photoassimilate Distribution Plants and Crops Source-Sink Relationships. Routledge; 2017. p. 501–518.

85. Akyol S, Alatas B. Plant intelligence based metaheuristic optimization algorithms. Artificial Intelligence Review. 2017;47(4):417–462.

86. Depuydt S. Arguments for and against self and non-self root recognition in plants. Frontiers in plant science. 2014;5:614.

87. Jiang J, Moore JA, Priyadarshi A, Classen AT. Plant-mycorrhizal interactions mediate plant community coexistence by altering resource demand. Ecology. 2017;98(1):187–197.

88. Chaiwanon J, Wang W, Zhu JY, Oh E, Wang ZY. Information integration and communication in plant growth regulation. Cell. 2016;164(6):1257–1268.

89. Sadeghi A, Mondini A, Del Dottore E, Mattoli V, Beccai L, Taccola S, et al. A plant-inspired robot with soft differential bending capabilities. Bioinspiration & biomimetics. 2016;12(1):015001.

B

Time after transfer (h)